scientific reports

Check for updates

OPEN

Multispectroscopic and computational insights into amyloid fibril formation of alpha lactalbumin induced by sodium hexametaphosphate

Nasser Abdulatif Al-Shabib[1]✉, Javed Masood Khan[1]✉, Ajamaluddin Malik[2], Md Tabish Rehman[3], Abdulaziz Alamri[2], Vijay Kumar[4], Per Erik Joakim Saris[5]✉, Fohad Mabood Husain[1] & Mohamed F AlAjmi[3]

The impact of sodium hexametaphosphate (SHMP) on the aggregation behavior of α-lactalbumin (α-LA) was studied at pH 7.4 and 2.0. Turbidity measurements showed a concentration-dependent aggregation of α-LA at pH 2.0 in the presence of SHMP, while no aggregation was observed at pH 7.4. Light scattering (LS) and Thioflavin-T (ThT) data revealed that the aggregation was rapid, following nucleation-independent pathways. In other kinetics experiments such as turbidity and ThT confirmed that SHMP-induced α-LA aggregation was dependent on SHMP concentration rather than incubation time. Once formed, the aggregates remained unchanged for up to five days. Intrinsic fluorescence studies indicated conformational changes in α-LA upon SHMP addition, and dye-binding assays with ThT and Congo Red demonstrated the formation of amyloid-like aggregates. Far-UV circular dichroism (CD) data suggested a structural transition from α-helical to β-structures in α-LA in the presence of SHMP at pH 2.0. Molecular docking studies confirmed stronger interactions between α-LA and SHMP at pH 2.0 (ΔG = −6.2 kcal/mol) compared to pH 7.4 (ΔG = −5.3 kcal/mol), driven by electrostatic forces and hydrogen bonding. These results suggest that SHMP induces amyloid-like aggregation of α-LA, particularly at acidic pH.

Keywords Amyloid fibril, Protein conformation, Stability, Alpha-lactalbumin, Sodium hexametaphosphate, ThT

Abbreviations

SHMP	Sodium hexametaphosphate
α-LA	Alpha-lactalbumin
ThT	Thioflavin T
CR	Congo red

Sodium hexametaphosphate (SHMP) is a common food additive frequently used in our diet. SHMP is present in many foods purchased from supermarkets and e-commerce. It is used in several industries, such as the food, chemical, textile, cosmetics, and pharmaceutical industries. In the food manufacturing process, polyphosphate was added to improve food qualities such as texture, tenderness, and water-holding capacity[1]. In the food industry, SHMP is frequently utilized as a thickening, stabilizing, and emulsifying ingredient. SHMP is mainly used in food to prevent food deterioration, inhibit the growth of microbes in food, and extend the shelf life of foods[2,3]. SHMPs have several health advantages. It can lower cholesterol, minimize inflammation, and reduce the risk

[1]Department of Food Science and Nutrition, Faculty of Food and Agricultural Sciences, King Saud University, P.O. Box 2460, Riyadh 11451, Saudi Arabia. [2]Department of Biochemistry, College of Science, King Saud University, Riyadh, Saudi Arabia. [3]Department of Pharmacognosy, College of Pharmacy, King Saud University, Riyadh, Saudi Arabia. [4]Himalayan School of Biosciences, Swami Rama Himalayan University, Jolly Grant, Dehradun , Uttarakhand 248016, India. [5]Department of Microbiology, Faculty of Agriculture and Forestry, University of Helsinki, Helsinki, Finland. ✉email: nalshabib@ksu.edu.sa; jmkhan@ksu.edu.sa; per.saris@helsinki.fi

of cardiovascular disease. Additionally, it could reduce the chance of kidney stones, enhance bone health, and improve digestion[4,5]. SHMP is also recognized to have potential negative effects in addition to its positive effects, such as nausea, vomiting, diarrhea, abdominal pain, and constipation. Moreover, it may result in an electrolyte imbalance, which may induce weariness, weakness, and cramping in the muscles. SHMPs are generally thought to be nontoxic, but some authors have reported that consuming large amounts of SHMPs through the diet can result in hypocalcemia and renal damage from the buildup of calcium phosphate in the kidneys[6,7]. Due to mixed opinions about the safety of SHMP, the European Commission (EC) asked the European Food Safety Authority (EFSA) to reassess the safety of food additives that were previously approved by the Union before 2009 (257/2010/EU), including SHMP, because of the high use of polyphosphate in food processing. Furthermore, phosphate content has not been mentioned in labeled processed foods like processed fish, soft drinks, and bakery products as a result of the above, various governmental agents regulate the permissible limits of inorganic phosphates in different types of foods as additive items[8].

Food proteins are an essential component of people's daily diets. Food proteins have a high biological value and high nutritional value. It was reported that SHMP has a high tendency to interact with protein molecules[9]. The SHMP molecules exhibit six evenly distributed molecules and can bind with calcium ions[10]. SHMP is a good calcium chelator and can bind three calcium atoms per SHMP molecule[11]. Many proteins and peptides can self-assemble into supramolecules and form amyloid fibrils[12]. These fibrils are linked to more than 30 human disorders, including Parkinson's disease and Alzheimer's disease[13]. Despite their importance in disease, amyloid fibril structures are useful in food processing, nanotechnology, biomedicine, and materials science. Understanding the mechanisms that control and modulate the processes of protein amyloid fibrillation is thus crucial and will have implications in many areas of contemporary scientific research. Amyloid fibril formation has been observed for a wide range of proteins, including those that are not known to generate amyloid fibrils in vivo[14]. Interestingly, the basic amino acid sequences of these amyloid fibril-forming proteins vary significantly, but all share common structural characteristics[15]. The amyloid fibrils are composed of β-strands arranged in an orderly fashion, positioned perpendicular to the axis of the fibril[16]. Amyloid fibrils are formed under both in vivo and in vitro conditions. Several intrinsic and extrinsic factors have been reported to stimulate the amyloid fibrillation process[17]. However, it has been reported that many small natural and synthetic molecules induce amyloid fibrillation in proteins under specific conditions[18,19].

The interaction and amyloid fibrillation mechanism between SHMP and alpha-lactalbumin (α-LA) under both low and neutral pH conditions were explored in this study. Alpha-lactalbumin (α-LA) is a globular metal-binding milk protein and a major constituent of human whey proteins[20]. α-LA has a large α-helical domain and a smaller domain primarily composed of beta structures[21]. These two domains are linked by a calcium-binding loop. The α-LA possesses antibacterial and antiviral activities[22]. The partially unfolded α-LA interacts with lipids and forms a complex, which is highly cytotoxic to many types of cancer cells[23]. α-LA has high water solubility over a wide pH range (2.0–9.0) and heat stability, making it suitable for use in beverages, particularly formula milk. Thus, the significance of α-LA for human health has been investigated worldwide. Several studies have been published on the unfolding, stability, and aggregation of α-LA[24,25]. The transformation of α-LA into a partially unfolded conformation is required for fibril formation, whereas a rigid (but flexible) structure may form amorphous aggregates[26].

SHMP and α-LA are present together in many food preparations, so we were interested to examine the effect of SHMP on the conformations of α-LA, at different pH levels. It was also reported that SHMP tends to interact with proteins and modify their structures, but how SHMP influences the solubility, structural integrity, and stability of α-LA whey protein has not been reported. Only our group recently published two research articles and reported that SHMP induces aggregation in hen egg white lysozyme and denatures the digestive enzyme trypsin[27,28]. Nevertheless, it is unclear how SHMP induces amyloid fibrils in whey food proteins. In the present study, we investigated the effect of SHMP on α-LA aggregation. We found that SHMP induces the formation of amyloid fibrils in α-LA, at acidic pH. The current study clarified the mechanisms by which SHMP induces amyloid fibrillation in α-LA at acidic pH and the factors that trigger this process. The formation of amyloid fibrils in the α-LA protein poses a serious concern to food safety because it may have a negative effect on human health and nutrition.

Materials and methods

Materials

Lyophilized powders of bovine α-LA and SHMP were purchased from Sigma Aldrich Co. (St. Louis, MO, USA). All other chemicals required were of analytical grade. Millipore filters with a pore size of 0.22 µm were purchased from Millipore Corp. Water from a Milli-QUF-Plus purification system was used for the preparation of all buffers.

Preparation and quantification of stocks of α-LA and SHMP

A stock solution of α-LA was prepared by dissolving it in 20 mM phosphate buffer at pH 7.4, and the dissolved solution was filtered through a 0.22 µm Millipore filter. The concentrations of α-LA were measured via a Cary 60 UV–visible spectrophotometer by measuring the absorbance at 280 nm, and the concentrations were calculated with the help of a molar extinction coefficient[29] of 28,500 M^{-1} cm^{-1}. A fresh stock of SHMP was prepared at 100 mM via wt./v. in Milli-Q water. The buffer 20 mM glycine-HCl pH 2.0 and sodium phosphate pH 7.4 were prepared for the study.

Turbidity of α-LA treated with SHMP samples

The effect of different concentrations of SHMP (0.0 to 5.0 mM) on α-LA was observed at pH 7.4 and 2.0, and changes were measured by measuring the absorbance at 350 nm with a Carry 60 UV–visible spectrophotometer

(Agilent Technologies). The changes in turbidity at 350 nm were recorded for α-LA without and with different concentrations of SHMP at both pH values. The changes in turbidity were plotted with respect to increasing concentrations of SHMP at pH 7.4 and 2.0. The concentrations of α-LA were fixed at 0.2 mg mL^{-1} for every sample.

SHMP-induced α-LA aggregation kinetics

The kinetics of SHMP-induced α-LA aggregation at pH 7.4 and 2.0 were determined by using right-angle light scattering (LS) measurements. The kinetics were measured by a Carry Eclipse spectrofluorometer by monitoring the change in light scattering at 350 nm after excitation at 350 nm. α-LA (0.2 mg mL^{-1}) was treated with different doses of SHMP at pH 2.0, and the effects were measured with respect to time (s). The LS intensity at 350 nm was recorded in a 3 mL cuvette with a 1.0 cm path length. The excitation and emission wavelengths were maintained at 350 nm with slit widths of 1.5 and 2.5 nm, respectively. For LS kinetics, the light scattering at 350 nm was recorded for 200 s without SHMP, different doses of SHMP were added, and the data were collected another 200 s after every addition.

The change in the tertiary structure of α-LA was measured by intrinsic fluorescence

We measured the changes in the tertiary structure of α-LA in response to different concentrations of SHMP by utilizing a Carry Eclipse spectrofluorometer. Excitation at 295 nm was used to measure the intrinsic fluorescence of α-LA treated with different SHMP at room temperature and pH 2.0. Emission spectra were recorded between 300 and 450 nm. All the samples were prepared using a fixed concentration of 0.2 mg mL^{-1} α-LA, and all the samples were incubated overnight before measurement. All the samples were scanned in triplicates. The excitation and emission slit widths were held at 2.5 and 5 nm, respectively.

ThT fluorescence measurement of SHMP-induced α-LA

ThT was dissolved in Milli-Q water and then filtered through a 0.22 µm syringe filter to make the stock solution. The ThT concentration was determined using an extinction coefficient of 36,000 M^{-1} cm^{-1} at 412 nm[30]. The ThT fluorescence was measured by a Carry Eclipse spectrofluorometer in a 1 mL cuvette. To quantify ThT fluorescence, the α-LA samples (0.2 mg mL^{-1}) were first incubated in various SHMP concentrations overnight at pH 2.0. After that, 10 µM ThT was added, and the mixture was incubated for an additional 30 min in the dark. The ThT fluorescence of all the samples was measured after excitation at 440 nm, and the emission spectrum was recorded from 450 to 650 nm. The excitation and emission slit widths were set to 2.5 and 5.0 nm respectively in this experiment.

Aggregation kinetics were monitored by ThT fluorescence

Aggregation reactions were set up in 20 mM glycine-HCl buffer pH 2.0 in the presence or in the absence of different mM of SHMP. ThT fluorescence kinetics were monitored under various conditions using 0.2 mg mL^{-1} α-LA and various concentrations of SHMP at pH 2.0. These conditions were as follows: (1) α-LA without SHMP in pH 2.0 buffer (control), (2) only buffer (control), (3) α-LA with 0.01, 0.07, 0.2 and 1.0 mM SHMP at the same pH. In all these samples, ThT was present at a concentration of 10 µM. The ThT fluorescence intensity was measured as a function of time in a 1 cm path length (3 mL) cuvette on Carry Eclipse spectrofluorometer, with excitation and emission wavelength fixed at 440 and 485 nm, respectively, using excitation and emission slit widths of 2.5 and 5 nm, respectively. The change in fluorescence intensity was measured with respect to time in seconds.

Congo Red (CR) binding assay

The 20 mM CR stock solution was produced in Milli-Q water and filtered. The concentration of the CR stock solution was determined spectrophotometrically using an extinction coefficient of 45 000 M^{-1} cm^{-1} at 498 nm. The fixed concentration of α-LA (0.2 mg mL^{-1}) was incubated with certain concentrations of SHMP (0.2, 0.5, and 1.0 mM) at pH 2.0 overnight. The next day, aliquots of CR (10.0 µM) were mixed with the above-treated samples and incubated for 15 min at room temperature in the dark. The absorbance spectra were recorded between 300 and 800 nm by a Carry 60 UV –visible spectrophotometer (Agilent Technologies) in a 1 cm path length cuvette at room temperature. The data were expressed after subtracting the appropriate blank.

Far-UV CD measurements

The CD measurements were carried out on a Chirascan Plus spectropolarimeter (Applied Photophysics, UK) with a thermostatically controlled cell holder. α-LA (0.2 mg mL^{-1}) was incubated without and with different concentrations of SHMP at pH 2.0 and left overnight. The next day, the experiments were carried out at room temperature, and the spectra were scanned in the range of 200–250 nm in a cuvette with a 0.1 cm path length. Each spectrum was an average of three scans. The spectra were smoothed by the Savitzky–Golay method.

All CD spectra were measured at room temperature. All the data were processed in Mean Residual Ellipticity (MRE) as described in our published reports[31]. The percent secondary structure was calculated by the K2D2 method.

Molecular docking

To explore the interaction between SHMP and α-LA, we utilized a molecular docking approach employing AutoDock VINA within PyRx following established protocols[32]. Initially, the chemical structure of SHMP was drawn using ChemSketch and saved in .pdf format. The protonation states of SHMP at pH 2.0 and pH 7.4 were assigned using Avogadro[33]. Subsequently, the ligand was then loaded into PyRx, and its energy was minimized using the universal force field (UFF) and converted to pdbqt format using Open Babel[34]. The 3D coordinates

of α-LA (PDB ID: 3B0O) were obtained from the RCSB website. To prepare the protein structure for docking, nonessential water molecules and foreign molecules were removed, and missing hydrogen atoms were added at pH 2.0 and pH 7.4. Energy minimization was performed using the CHARMM36 force field[35]. For the molecular docking process, a grid box with dimensions of $35 \times 45 \times 45$ Å^3 was positioned at $12 \times 28 \times 13$ Å^3 with a spacing of 0.375 Å. Molecular docking was conducted using the Lamarckian Genetic Algorithm (LGA) coupled with Solis and Wets local search methods[36]. The ligands were assigned random initial positions, orientations, and torsions. Each docking run involved a maximum of 2.5×10^6 energy calculations, with a population size of 150, translational step of 0.2 Å, torsion steps of 5, and quaternions of 5. Following docking, the obtained results were analyzed, and the final figures were generated using Discovery Studio (Accelrys). The association constant (K_a) of SHMP for α-LA was computed by evaluating the docking energy (ΔG) using the relevant formula[37].

$$\Delta G = -RT \ \ln \ K_a$$

Where, R and T are the universal gas constant and temperature, respectively.

Results

Assessing the effect of SHMP on α-LA aggregation

α-LA aggregation was examined in the presence of SHMP at pH values of 7.4 and 2.0. The α-LA aggregation in the presence of SHMP was measured by turbidity at 350 nm. A measurement of the turbidity of a solution can reveal important details such as the protein's solubility, clarity, and aggregation. Figure 1A demonstrated the turbidity profile of α-LA at 350 nm in response to increases in SHMP concentration at pH 7.4 and 2.0. In the control experiment, different concentrations of SHMP at pH 2.0 without protein were used. The turbidity of α-LA treated with 0.03 mM to 5.0 mM SHMP at pH 2.0 significantly increased. The turbidity increase was shown to be dose-dependent between 0.03 mM and 1.0 mM SHMP and plateau was found at above 1.0 mM. However, when identical experiments were carried out at pH 7.4, turbidity was not observed, and the absorbance was recorded at baseline for all SHMP concentrations. The turbidity profile of SHMP without protein was also measured to ensure that the SHMP did not form aggregates at pH 2.0. This measurement was regarded as a good control, and the likelihood of SHMP aggregation was eliminated. Turbidity analysis suggested that in the presence of varying concentrations of SHMP, ranging from 0.03 to 5.0 mM, α-LA formed aggregates at pH 2.0, and α-LA remained soluble (nonaggregated) at pH 7.4. Interestingly, when α-LA was treated with SHMP at concentrations less than 0.03 mM, it was found to be soluble and nonaggregated at pH 7.4 and 2.0.

Figure 1B, showed the turbidity at 350 nm of samples incubated with fixed α-LA concentration (0.2 mg mL^{-1}) and various SHMP concentrations at pH 2.0. The turbidity readings were recorded every day for 5 days. The turbidity profile indicated that when SHMP came into contact with α-LA, at pH 2.0, the turbidity increased quickly due to aggregate formation and remained constant for 5 days. Interestingly, the turbidity profile changes in response to the SHMP concentration. Less SHMP-containing samples had lower turbidity and vice versa.

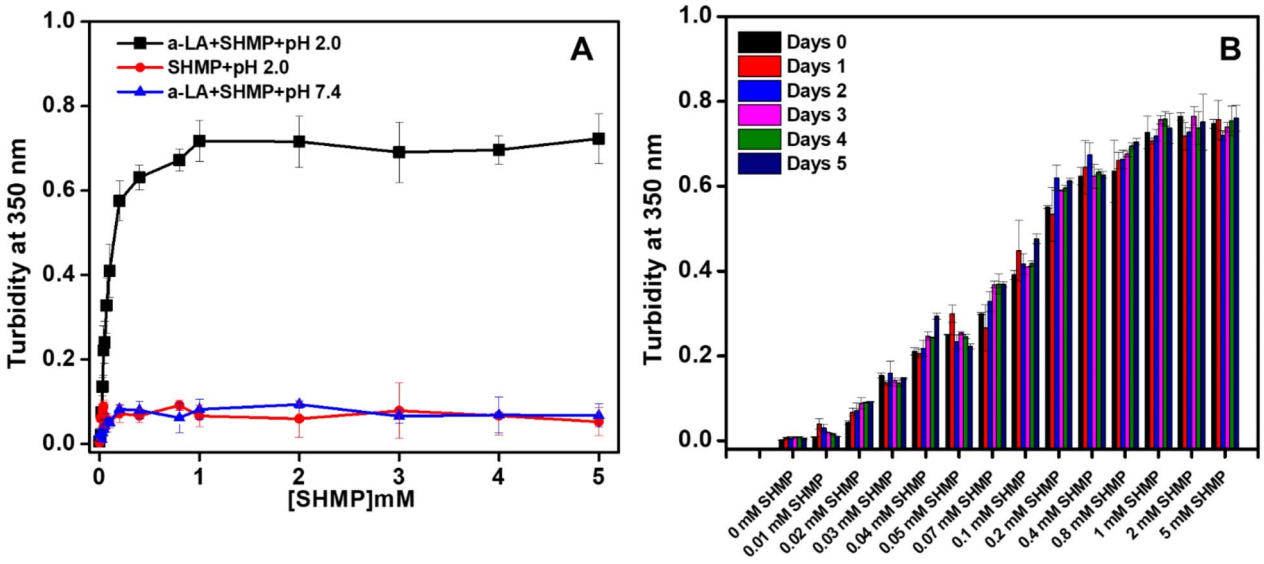

Fig. 1. (**A**) Effects of SHMP on α-LA aggregation at acidic pH. The turbidity of α-LA without and with different SHMP concentrations at pH 2.0 (black squares), pH 7.4 (blue triangles) was recorded by measuring the absorbance at 350 nm. The turbidity of SHMP alone at pH 2.0 (red circles) was measured as a control. (**B**) The Turbidity kinetics of α-LA were measured in the presence of different SHMP concentration (0–5 mM) after various incubation periods at pH 2.0. The α-LA concentrations were fixed at 0.2 mg mL^{-1} in all the samples. The α-LA and SHMP controls do not show any turbidity of its own over all the concentration range and incubation periods.

However, once the aggregates formed, the turbidity at 350 nm was unchanged. Turbidity levels were observed to be consistent over the period.

Kinetics of the SHMP-induced aggregation profile of α-LA

The aggregation profile of α-LA in the presence of SHMP was monitored by LS measurements. In LS measurements, the change in light scattering in response to time is frequently used to monitor the kinetics of protein aggregation. α-LA was treated with different concentrations of SHMP at pH 2.0, and variations in light scattering were observed in seconds, as shown in Fig. 2A. In these kinetics measurements, we used varying doses of SHMP and recorded light scattering at 350 nm for 200 s. At the same time, we administered another dose of SHMP and measured the scattering for an additional 200 s. At pH 2.0, no light scattering was observed for α-LA without SHMP, suggesting that α-LA did not form aggregates over a 200-second time scale. However, the light scattering increased 50 times as soon as a very low concentration (0.05 mM) of SHMP was added, reaching a plateau within 200 s of the scan. When another dose of SHMP (0.1 mM) was added to the same sample, the light scattering increased very strongly, and the reaction rapidly reached saturation. With further addition (0.2, 0.5, and 1.0 mM) of SHMP, the light scattering was almost equal to the light scattering of the 0.1 mM SHMP-treated samples. This kinetic behavior suggested that maximum aggregation occurred in the presence of 0.1 mM SHMP. According to the LS kinetics pattern. The aggregation that took place in the presence of SHMP was independent of the duration of nucleation, indicating that the lag phase was completely missing. When the α-LA monomer interacted with a specific concentration of SHMP, it immediately transformed into larger aggregates, with maximum aggregation observed in the presence of 0.1 mM SHMP.

Furthermore, the impact of salt on the kinetics of the sample containing 0.2 mg mL^{-1} of α-LA and 0.1 mM SHMP at pH 2.0 was observed, and the data are shown in Fig. 2B. The figure indicates that 0.1 mM SHMP does not affect nucleus-independent aggregation. However, when 50–500 mM NaCl is added, the reaction kinetics remain unchanged, and the light scattering is found to be similar to that observed before the addition of salts. NaCl was ineffective because it did not affect the aggregation caused by SHMP.

Intrinsic fluorescence study

Intrinsic fluorescence measurements provide valuable information about the position of aromatic amino acid residues, such as tyrosine (Tyr), tryptophan (Trp), and phenylalanine (Phe). The fluorescence intensity and the wavelength at peak intensity are sensitive indicators of protein conformational changes. These parameters serve as crucial tools for investigating processes related to protein folding, unfolding, and aggregation. Figure 3A shows the fluorescence emission spectra of α-LA recorded without and with increasing concentrations of SHMP at an excitation wavelength of 295 nm. α-LA without SHMP at pH 7.4 exhibited a significant fluorescence emission peak at 328 nm, which is very similar to a previously published report[38]. However, the fluorescence intensity of α-LA, at pH 2.0 remained unchanged, yet the wavelength maximum shifted toward the red region due to conformational changes. Figure 3B, showed the spectra of α-LA in the presence of 0.03 to 0.1 mM of SHMP, the fluorescence intensity was marginally lower than that of the sample at pH 7.4 and 2.0. Remarkably, the

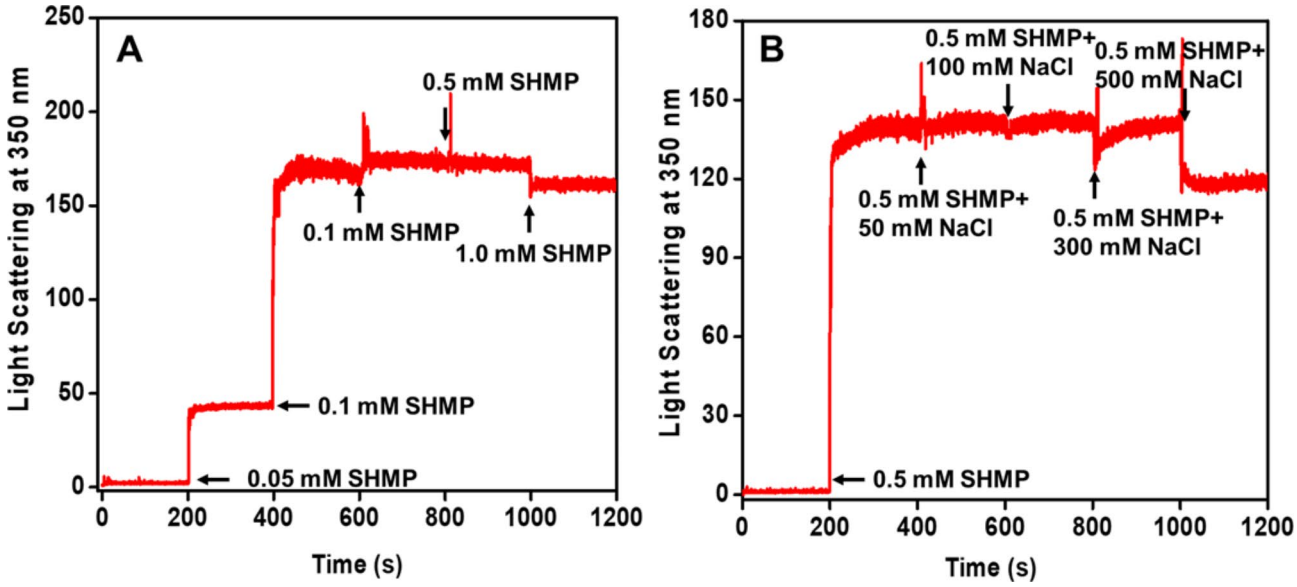

Fig. 2. (**A**) The aggregation kinetics of α-LA were monitored in the presence of SHMP at pH 2.0. (**A**) Light scattering of α-LA (0.2 mg mL^{-1}) without and with different concentrations of SHMP was measured at 350 nm. The different concentrations of SHMP were added every 200 s, and scattering was monitored continuously. (**B**) Effect of salt (NaCl) on the aggregation kinetics of SHMP-induced α-LA aggregates. The scattering of α-LA without and with 0.2 mM SHPM was scanned in the presence of different doses of salt, and different concentrations of salts were added every 200 s.

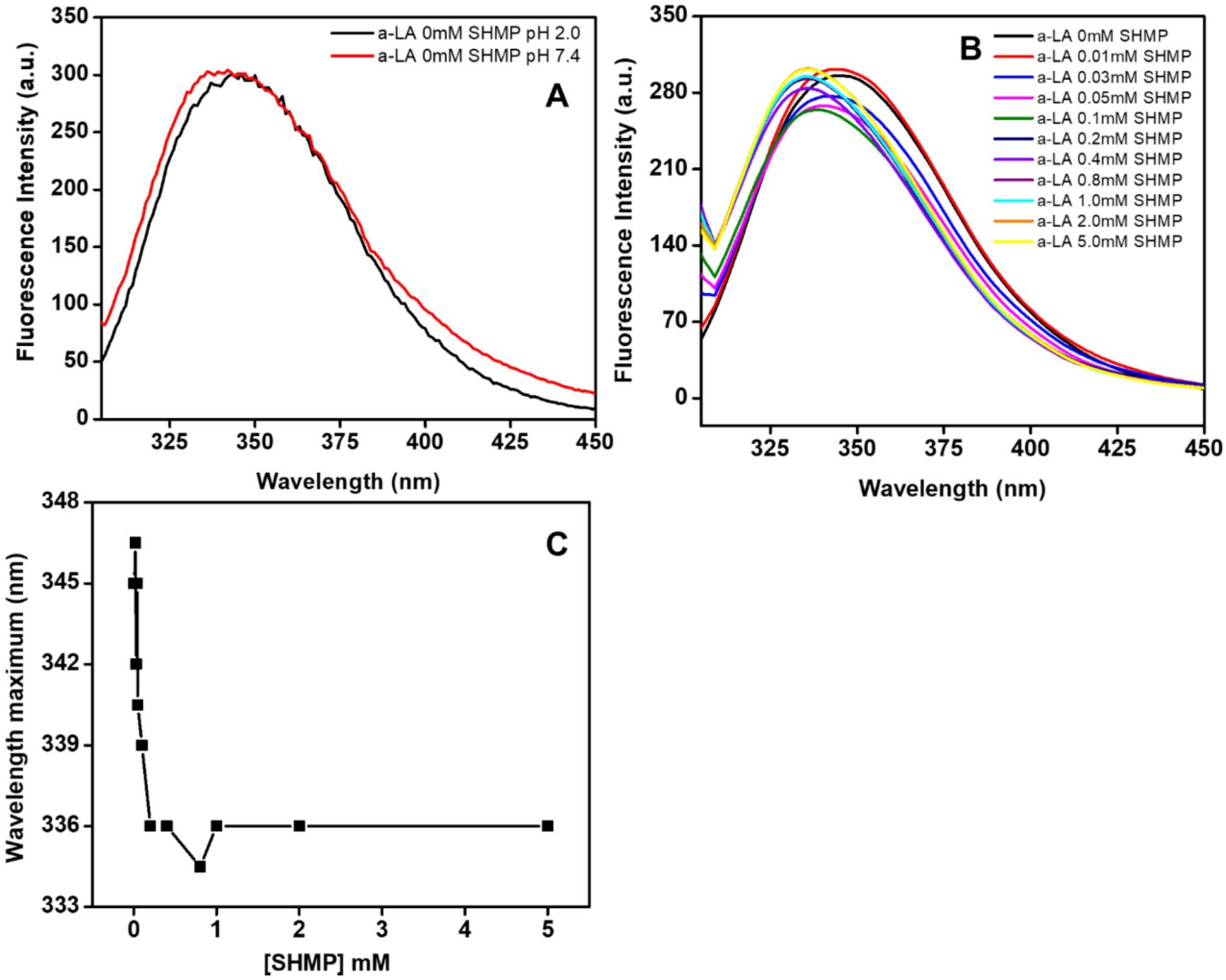

Fig. 3. (**A**) Intrinsic fluorescence of α-LA, at pH 7.4 (▬), and pH 2.0 (▬). (**B**) Intrinsic Trp fluorescence emission spectra (λex = 295 nm) of α-LA (0.2 mg mL^{-1}) without SHMP (▬), and in the presence of different concentrations of 0.01 (▬), 0.03 (▬), 0.05 (▬), 0.1 (▬), 0.2 (▬), 0.4 (▬), 0.8 (▬), 1.0 (▬), 2.0 (▬), and 5.0 (▬) mM SHMP at pH 2.0. (**C**) The wavelength maximum was plotted against SHMP in mM concentration at pH 2.0.

wavelength maximum shifted toward a blueshift. Upon the addition of SHMP concentrations ranging from 0.2 to 5.0 mM, the fluorescence intensity of α-LA reached almost the same level as native (pH 7.4) or unfolded (pH 2.0) α-LA. Additionally, a significant blue shift in the maximum wavelength was observed. Figure 3C and Table 1 exhibit the shifts in wavelength maximum in response to SHMP concentrations at pH 2.0. The data revealed that the wavelength maximum of α-LA undergoes a blue shift when exposed to a very low concentration of SHMP (0.02). The highest blue shift occurred when 0.2 mM SHMP was present. Nevertheless, the wavelength maxima remained constant beyond 0.2 mM SHMP. The decrease in fluorescence intensity with a blueshift in wavelength was indicative of a conformational change in α-LA. The formation of aggregates in the presence of SHMP at pH 2.0 resulted in these conformational changes.

The effect of SHMP on amyloid fibrillation of αLA using a thioflavin T (ThT) binding assay

We are interested in determining whether the aggregation that SHMP caused was fibrillar or amorphous in nature. ThT is a fluorescent dye that is frequently used to identify amyloid fibrils in solution. It has been observed that this dye binds selectively to the β-sheet structure that characterizes amyloid fibrils. When the thioflavin T (ThT) dye is in its free state or an aqueous solution, it exhibits little fluorescence. In this study, a ThT binding assay was carried out to examine the effects of different doses of SHMP on the fibrillation of α-LA, at pH 2.0. Figure 4A shows the ThT fluorescence spectra of αLA without and with different concentrations (0.01–5.0 mM) of SHMP at pH 2.0. ThT binding to α-LA was negligible both in the presence and absence of SHMP at concentrations less than 0.01 mM. However, a low ThT binding was observed at concentrations 0.03–0.1 mM SHMP, and ThT binding keeps on increasing above 0.1 mM and the maximum ThT binding was observed in the presence of 1.0 mM SHMP. In Fig. 4B, the ThT fluorescence intensity at 485 nm was plotted against every concentration of SHMP at pH 2.0. The figure demonstrated that the ThT fluorescence intensity at 485 nm grew slightly between

S.No.	Condition	Wavelength maximum (nm)
1	α-LA 0.0 mM SHMP at pH 2.0	345
2	α-LA 0.01 mM SHMP at pH 2.0	345
3	α-LA 0.02 mM SHMP at pH 2.0	345
4	α-LA 0.03 mM SHMP at pH 2.0	342
5	α-LA 0.05 mM SHMP at pH 2.0	340
6	α-LA 0.07 mM SHMP at pH 2.0	339
7	α-LA 0.1 mM SHMP at pH 2.0	336
8	α-LA 0.2 mM SHMP at pH 2.0	336
9	α-LA 0.4 mM SHMP at pH 2.0	334
10	α-LA 0.8 mM SHMP at pH 2.0	336
11	α-LA 1.0 mM SHMP at pH 2.0	336
12	α-LA 2.0 mM SHMP at pH 2.0	336
13	α-LA 5.0 mM SHMP at pH 2.0	336

Table 1. The wavelength maximum data were presented against different SHMP concentrations at pH 2.0.

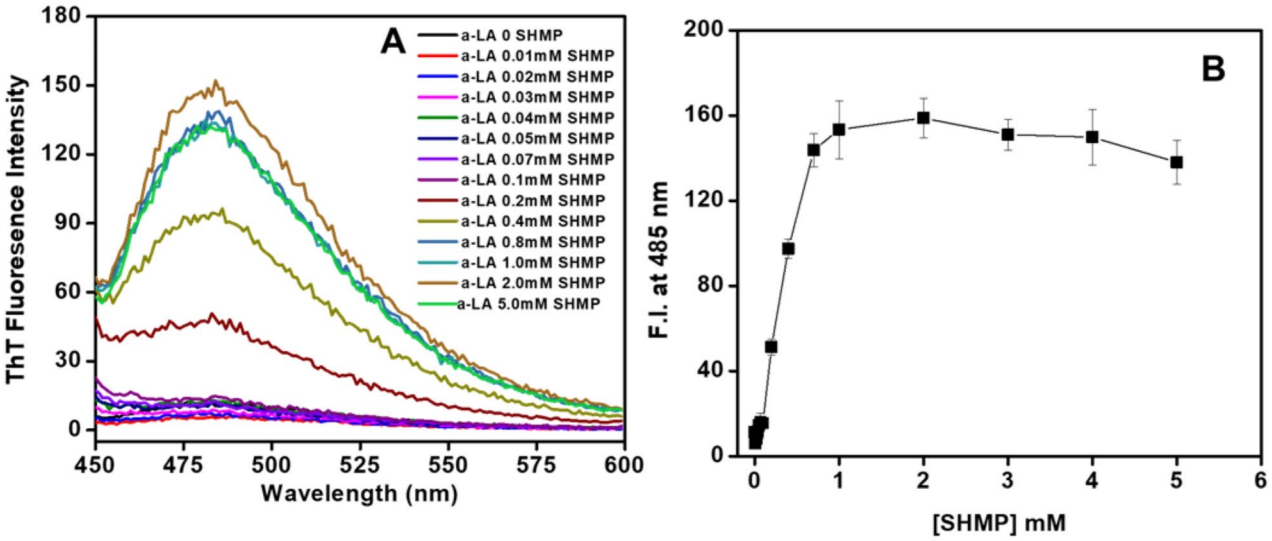

Fig. 4. (**A**) ThT fluorescence spectra of 0.2 mg mL^{-1} α-LA in the absence (▬) and presence of 0.01 (▬), 0.02 (▬), 0.03 (▬), 0.04 (▬), 0.05 (▬), 0.07 (▬), 0.1 (▬), 0.2 (▬), 0.4 (▬), 0.8 (▬), 1.0 (▬), 2.0 (▬) and 5.0 (▬) mM SHMP at pH 2.0. (**B**) Fluorescence intensity at 485 nm was plotted against SHMP at pH 2.0. The error bars represent the standard errors of the means estimated from at least three individual measurements.

0.03 and 0.1 mM and remained stable, but then increased above 0.1 mM until the ThT concentration reached 1.0 mM. After that, the intensity remained constant when the remaining concentrations of 2.0, 3.0, and 5.0 mM were present. The ThT fluorescence spectra and intensity at 485 nm indicated that the amyloid-type aggregates formed by SHMP in α-LA, at pH 2.0 are supported by the notable increase in ThT binding at concentrations above 0.1 mM SHMP.

Kinetics of SHMP-Induced α-LA aggregation monitored via ThT fluorescence

The changes in ThT fluorescence intensity at 485 nm with the time passage 0.0–300 s were used to analyze the aggregation of the α-LA with the exposure of various concentrations of SHMP at pH 2.0 shown in Fig. 5A. ThT is an excellent reporter dye which is used to identify the types of aggregates in a solution. The ThT fluorescence intensity was unchanged in the protein control (α-LA without SHMP), buffer control, and α-LA with 0.01 mM SHMP at pH 2.0 samples, indicating that the α-LA was soluble under the aforesaid circumstances and that there was no presence of micro and macro aggregates. However, ThT signals increased immediately as the α-LA was treated with 0.07, 0.2, and 1.0 mM SHMP, and the reaction reached saturation in just a couple of seconds without a noticeable lag phase. The ThT signals were higher at a 1.0 mM concentration compared to 0.2 mM, 0.07 mM which suggested that α-LA forming amyloid-like aggregates in response to the concentration of SHMP. Overall, the ThT kinetics study data suggest that SHMP-induced aggregates are kinetically very fast following non-nucleation-dependent phenomena and having amyloid fibril in the presence of certain concentrations of

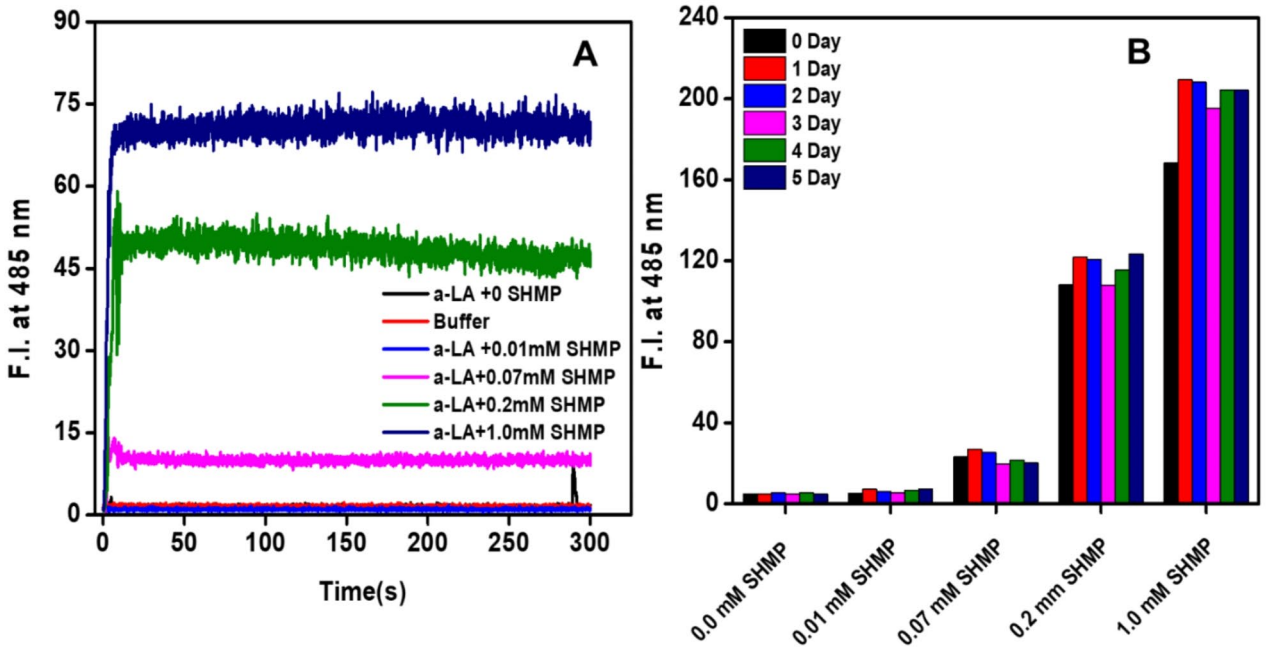

Fig. 5. Kinetics of SHMP-induced amyloid fibril formation, measured by ThT fluorescence: (**A**) Aggregation kinetics of α-LA (0.2 mg mL^{-1}) without (black) and with various concentrations 0.01 (blue), 0.07 (magenta), 0.2 (green), and 1.0 (navy blue) mM of SHMP at pH 2.0. The control was also measured without α-LA and SHMP (red) at pH 2.0. (**B**) The fluorescence intensity at 485 nm was plotted against different concentrations of SHMP on different days at pH 2.0.

SHMP. Similar aggregation kinetics were seen when 30 and 60 μM Aβ-(16–22) were incubated in pH 7.4 buffer and the aggregation reaction was found to be without the lag phase formation[39].

Figure 5B demonstrated the time-dependent aggregation kinetics in response to different SHMP concentrations, with measurements taken over several days. From the data, it was seen that for up to 0.01 mM SHMP treatments, the ThT signals were at baseline even up to 5.0 days incubation. However, ThT signals were shown to be higher at concentrations of 0.07, 0.2, and 1.0 mM of SHMP. Interestingly, the ThT signals were found to be the same at all times despite the signals that were recorded in the first days being a little bit lower in intensity. The results of these measurements suggest that the amyloid structure remained unchanged after its formation.

Congo Red (CR) binding

ThT has been primarily utilized in the detection of amyloid fibrils, and it is also capable of binding to other protein aggregates, such as protein oligomers. To confirm the presence of amyloid fibrils, a complementary assay, such as the CR binding assay, was used. The CR binding assay results are shown in Fig. 6. The maximum absorbance of the CR dye bound to α-LA in the absence of SHMP was observed at approximately 495 nm at pH 7.4. Since CR is also used as a pH indicator, the absorbance maximum of CR was slightly redshifted when α-LA was incubated at pH 2.0 without SHMP. Remarkably, the absorbance maximum was significantly redshifted (~ 50 nm) when α-LA was treated with 0.2, 0.5, and 1.0 mM SHMP at pH 2.0, indicating the presence of amyloid-like aggregates. The ThT and CR dye binding results indicated that SHMP at pH 2.0 induces the formation of amyloid-like aggregates in α-LA.

SHMP-induced changes in the secondary structure of α-LA

It has been proven that far-UV CD is the most effective spectroscopic technique for monitoring the conformational changes of proteins in solution. This study aimed to investigate the alterations in the secondary structure of α-LA, at pH 2.0 and 7.4 in the presence of varying concentrations of SHMP. The far-UV CD spectra were scanned in the presence of different concentrations of SHMP, and the spectra are presented in Fig. 7A,B. As shown in Fig. 7A,B, the far-UV CD spectra of α-LA, at pH 2.0 (A) and 7.4 (B) in the absence of SHMP exhibited negative ellipticity at 208 and 222 nm, consistent with findings reported in other publications[40]. When very low concentrations below 0.015 mM were added at pH 2.0 (Fig. 7A), there was a slight increase in negative ellipticity, indicating that α-LA gained additional secondary structure. On the other hand, when α-LA was treated with 0.02, 0.07, 0.2, and 0.3 mM SHMP at the same pH, a pronounced decrease in negative ellipticity was recorded. Interestingly, both negative ellipticity peaks disappear, and a single negative ellipticity peak emerges at a higher wavelength, specifically at 225 nm. The appearance of a single peak at 225 nm indicated that the α-LA secondary structure had completely transformed into a β-structure, a sign of the development of an amyloid-like structure. The effect of SHMP concentrations from 0.0 to 0.07 mM on α-LA was also observed at pH 7.4, as shown in

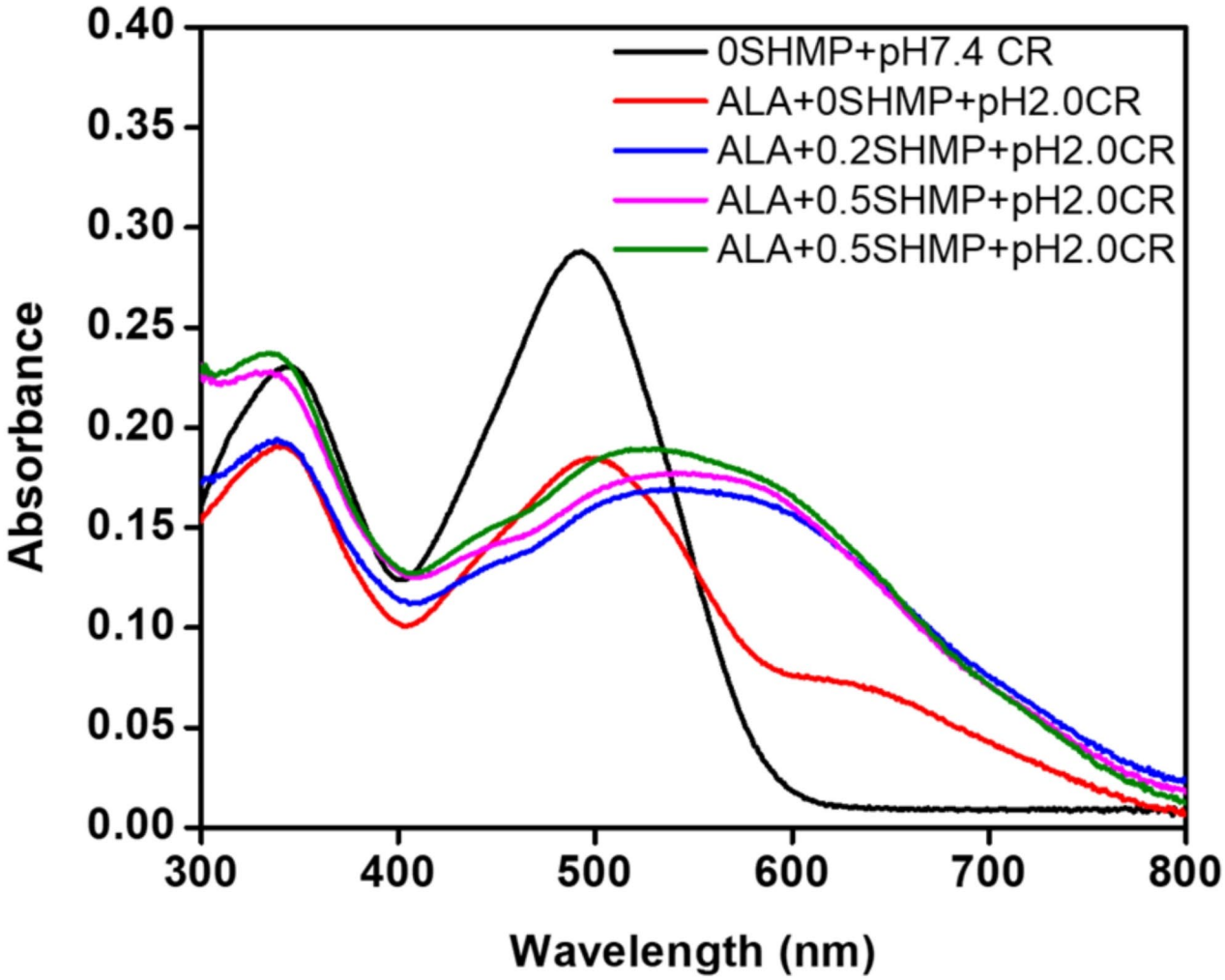

Fig. 6. Congo Red (CR) binding was performed to detect the amyloid fibrils in solution. The absorbance spectra of α-LA (0.2 mg mL^{-1}) were obtained under different conditions, such as CR binding at pH 7.0 (▬) and pH 2.0 (▬) in the presence of 0.2 (▬), 0.3 (▬), and 0.5 (▬) mM SHMP at pH 2.0. A fixed amount of CR (10 μM) was added to both the aggregated and nonaggregated samples and incubated for 30 min in the dark prior to the measurements.

Fig. 7B. The figure clearly indicates that the negative ellipticity slightly increased, and the peak position remained unchanged. This suggests that α-LA gained more secondary structure at pH 7.4. The details change in secondary structure conversion in response to SHMP at both pHs was presented in Table 2. The table itself reflected that α-LA gained more percent secondary structure at pH 7.4 at all SHMP concentrations. On the other hand, α-LA percent secondary structure increased at concentrations of 0.01 and 0.015 mM SHMP, and significant conversion occurred at concentrations of 0.02, 0.07, 0.2, and 0.3 mM SHMP at pH 2.0. Under these conditions, the percentage of α-helix almost disappeared and the overall amount of β-structure increased.

Analysis of the interaction between α-LA and SHMP at pH 2.0

In this investigation, we utilized a molecular docking approach to assess the binding affinity of SHMP for α-LA. Our findings demonstrated that the ligand effectively bound to α-LA, displaying a binding energy of −6.2 kcal mol^{-1} (Table 3), as illustrated in Fig. 8. The stability of the α-LA-SHMP complex predominantly relies on electrostatic interactions and hydrogen bonding. Specifically, SHMP formed four electrostatic interactions with Lys58 (two interactions), Tyr103, and His107. In addition, SHMP interacted with α-LA through eight hydrogen bonds with Glu49 (four interactions), Tyr103, Trp104, and Lys108 (two interactions) (Fig. 8; Table 3). These interactions collectively contributed to the stability of the SHMP and α-LA complex. The association constant (K_a) for the SHMP-α-LA complex at pH 2.0 was estimated to be 3.53×10^4 M^{-1}.

Analysis of the interaction between α-LA and SHMP at pH 7.4

In this study, a molecular docking approach was employed to evaluate the binding potential of SHMP to α-LA. The results revealed that SHMP bound to α-LA, exhibiting a binding energy of −5.3 kcal mol^{-1} (Fig. 9; Table 3).

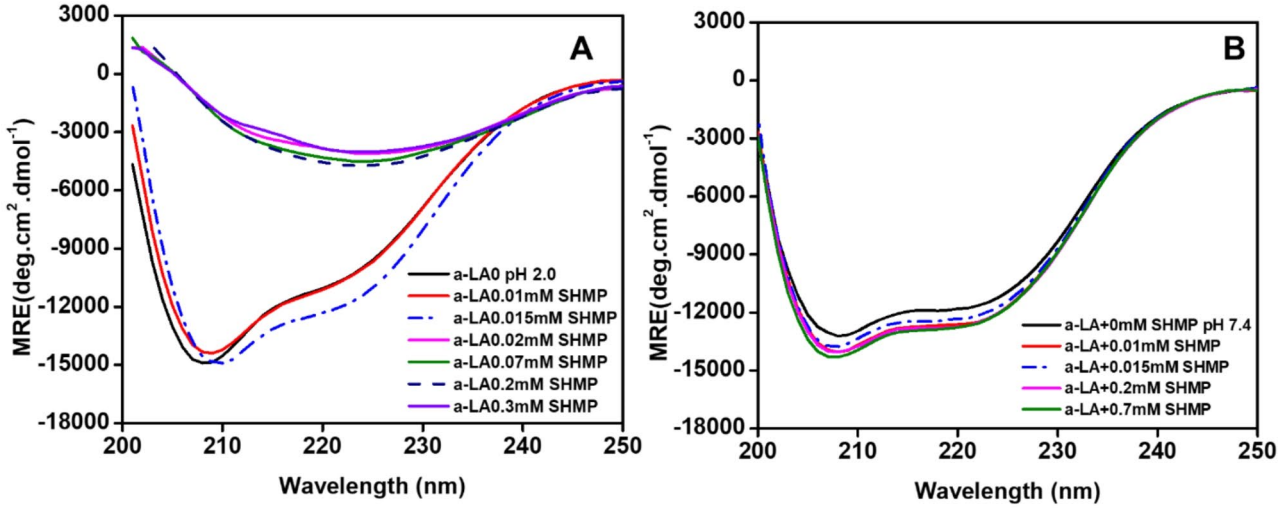

Fig. 7. Changes in the secondary structure of α-LA in response to SHMP at pH 2.0 and 7.4. (**A**) Far-UV CD spectra of α-LA in the absence (▬) and presence of 0.01 (▬), 0.015 (▬●▬), 0.02 (▬), 0.07 (▬), 0.2 (▬ ▬), and 0.3 mM (▬) SHMP at pH 2.0. (**B**) Far-UV CD spectra of α-LA in the absence (▬) and presence of 0.01 (▬), 0.015 (▬●▬), 0.02 (▬), and 0.07 (▬) mM SHMP at pH 7.4. In all the samples, the α-LA concentration was fixed at 0.2 mg mL^{-1}.

S. no.	Conditions	pH 7.4		pH 2.0	
		% α-helix	% β-sheet	% α-helix	% β-sheet
1	α-LA + 0 mM SHMP	26.47	19.07	25.35	24.96
2	α-LA + 0.01 mM SHMP	43.29	10.79	25.35	24.96
3	α-LA + 0.015 mM SHMP	43.29	10.79	27.17	17.88
4	α-LA + 0.02 mM SHMP	43.29	10.79	1.76	47.42
5	α-LA + 0.07 mM SHMP	43.29	10.79	1.76	47.42
6	α-LA + 0.2 mM SHMP	43.29	10.79	1.76	47.42
7	α-LA + 0.3 mM SHMP	43.29	10.79	1.76	47.42

Table 2. The change in the percent secondary structure of α-LA under different conditions was calculated by K2D2 methods.

pH value	Electrostatic interactions	Hydrogen bonding	van der Waals' interactions	Docking energy (kcal mol^{-1})	Binding affinity (M^{-1})
2.0	Lys58*, Tyr103, His107	Glu49$^{\#}$, Tyr103, Trp104, Lys108*	–	−6.2	3.53×10^4
7.4	–	Ser64, Gln65, Asp78	Ile41, Thr48, Tyr50, Ser63, Leu81,	−5.3	0.77×10^4

Table 3. Molecular docking parameters for the interaction between α-LA and SHMP at different pH values.

The stability of the α-LA and SHMP complex primarily relies on three hydrogen bonds with Ser64, Gln65, and Asp78. Additionally, van der Waals interactions were observed between SHMP and specific amino acid residues of α-LA, including Ile41, Thr48, Tyr50, Ser63, and Leu81. These interactions further contributed to the stability of the SHMP-α-LA complex. The association constant (K_a) for the SHMP-α-LA complex at pH 7.4 was estimated to be 0.77×10^4 M^{-1}, which is approximately 4.5 times lower than that at pH 2.0.

The computational findings corroborate the experimental results indicating a stronger binding affinity between SHMP and α-LA, at pH 2.0 than at pH 7.4. At pH 7.4, both α-LA and SHMP carry negative charges, potentially leading to repulsion at the binding site. Nevertheless, there is still an interaction between SHMP and α-LA at neutral pH, although with reduced affinity compared to acidic conditions. Conversely, at pH 2.0, α-LA is positively charged, while SHMP is negatively charged, facilitating stronger electrostatic interactions between the two molecules.

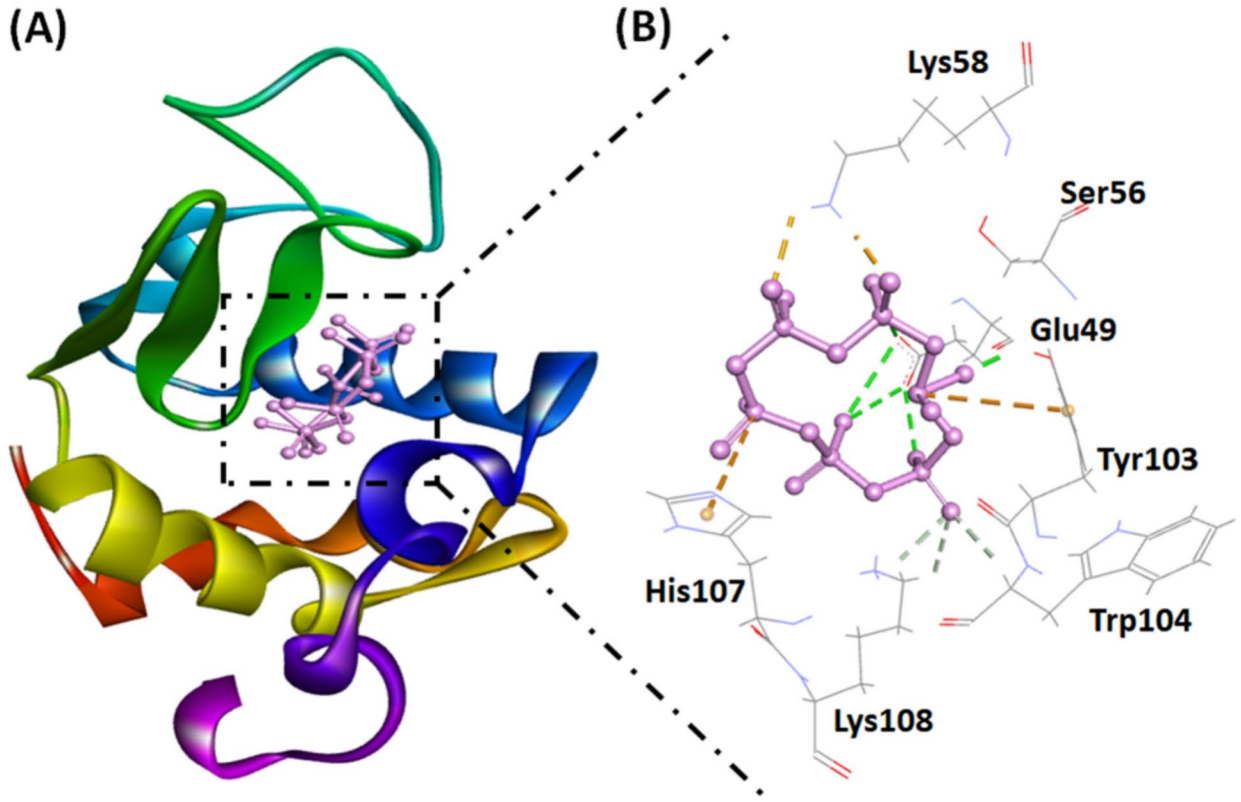

Fig. 8. (**A**) Molecular docking image illustrating the interaction between SHMP and the α-LA cavity. (**B**) The molecular interaction between SHMP and α-LA highlights electrostatic interactions (orange dashed lines) and hydrogen bonds (dark green dashed lines).

Discussion

In this study, we examined the mechanism of interaction between SHMP and α-LA at two pHs i.e., physiological and acidic pH. We are also interested to identify aggregate formation and its nature. SHMP is the alkali salt of a series of polymetaphosphoric acids (acids formed by the polymerization of phosphate groups). Excessive intake of phosphate leads to elevated blood phosphate levels, which can result in severe illness. It has been reported that inorganic phosphates are incorporated into processed foods to improve their texture, juiciness, and other desirable characteristics[41]. In the food processing industry, inorganic phosphates partially substitute for sodium chloride, particularly in the dairy and meat sectors. The goal of this substitution is to improve the flavor and texture of the finished product, among other qualities[42]. The phosphate group of SHMP has a strong tendency to interact with the oppositely charged amino acids of proteins. It has already been reported that negatively charged molecules such as sodium dodecyl sulfate, phospholipid phosphates, and polyphosphates interact with proteins and induce amyloid fibril[43–45]. It has not been reported that SHMP induces amyloid fibrils in dietary proteins, although it also contains a negatively charged phosphate group. These two molecules (protein and SHMP) are present together in our food, so it is interesting to investigate the conformational changes due to the interaction between SHMP and α-LA.

Our results clearly indicated that α-LA forms amyloid-like aggregates in the presence of specific concentrations of SHMP at acidic pH, while at pH 7.4, α-LA is soluble in the presence of all SHMP concentrations. At an acidic pH, α-LA usually becomes positively charged due to the protonation of cationic amino acids. This suggests that the potential interaction between positively charged α-LA and negatively charged SHMP may involve both electrostatic and hydrophobic forces. However, at pH 7.4, α-LA has an overall negative charge, so SHMP was unable to interact due to electrostatic repulsion. It has been reported that electrostatic and hydrophobic interactions play important roles in protein aggregation and amyloid fibrillation[46,47].

The turbidity results indicated that SHMP induces aggregation in α-LA, at pH 2.0 and that this aggregation is dependent on the SHMP concentration. As shown in Fig. 1, aggregation in α-LA is induced by SHMP at concentrations greater than 0.01 mM at pH 2.0, and the extent of aggregation is dependent upon the concentration of SHMP. Less aggregation was observed at lower concentrations, whereas larger aggregates formed at higher concentrations. The turbidity profile indicated that α-LA and SHMP interacted which leads to protein aggregation. Similar SHMP-induced turbidity profiles were also observed with HEWL at pH 7.0 and trypsin at pH 6.0[48,49]. The influence of SHMP on aggregation kinetics was also tested. Figures 2 and 5 showed that SHMP induced aggregation kinetically very quickly without the lag phase. Usually, aggregation kinetics follow a sigmoidal curve, including nucleation, rapid growth, and saturation phases but in some cases, non-

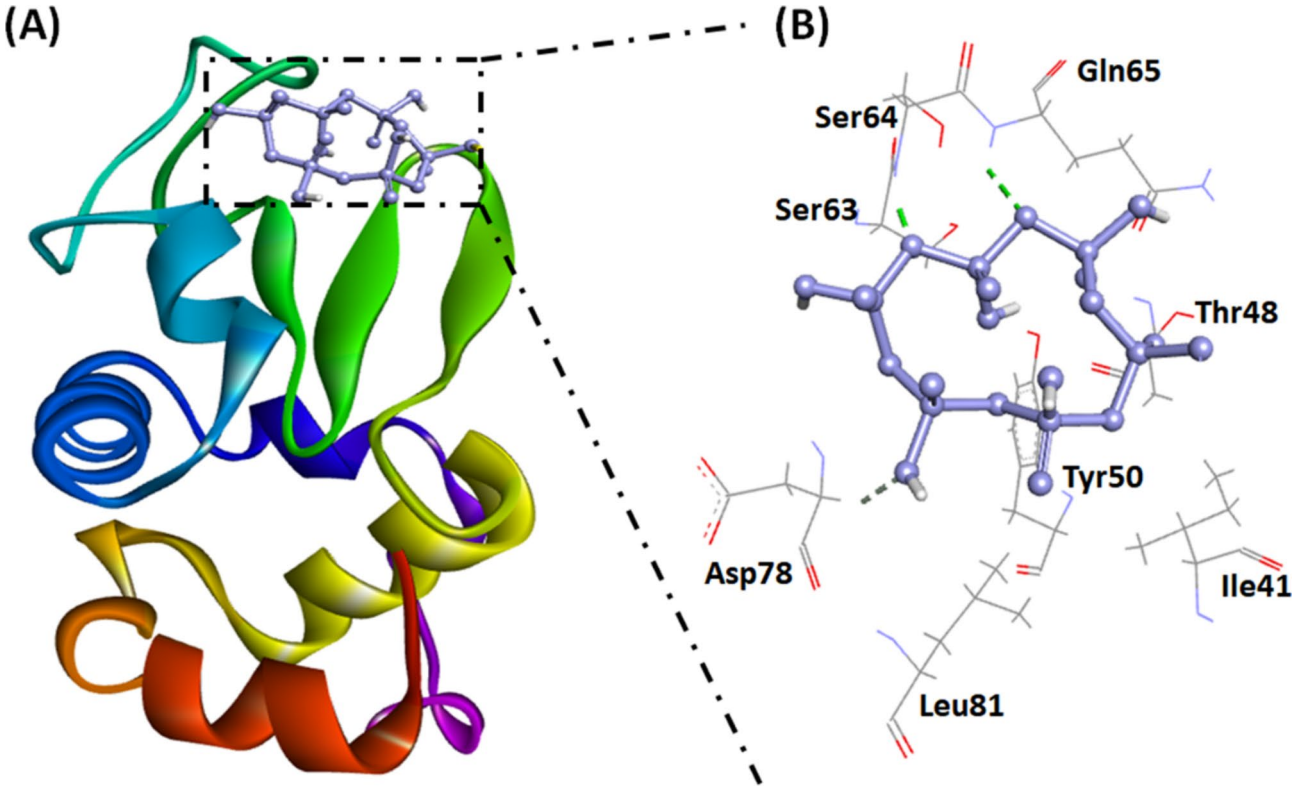

Fig. 9. (**A**) Molecular docking image illustrating the interaction between SHMP and the α-LA surface at pH 7.4. (**B**) Molecular interaction between SHMP and α-LA showing electrostatic interactions (orange dashed lines) and hydrogen bonds (dark green dashed lines).

nucleation amyloid fibrillation also reported[39,50]. The aggregation kinetics provide valuable insight into the dynamic process of protein aggregation. In this work, we observed that the LS and ThT kinetics results showed that the aggregation reaction was remarkably rapid, reaching saturation within a few seconds. This suggests that the aggregation mechanism is nucleus-independent. When the α-LA monomers come into contact with SHMP, they transform into bigger aggregates or amyloid fibril formation. Similar LS and ThT kinetics trends were also observed with bromophenol blue and SHMP insulin, HEWL, and trypsin at different pHs[48,49,51]. Both the kinetics (LS and ThT) and turbidity observations suggested that certain concentrations of SHMP induce aggregation and amyloid formation in α-LA. This study showed that once SHMP-induced aggregates/amyloids formed they remained stable for several days (Figs. 1B and 5B).

We further explored the conformational changes in the tertiary structure in the presence of SHMP. At pH 2.0, the intrinsic fluorescence spectrum of α-LA redshifted due to unfolding. However, the addition of 0.03 mM and above concentrations of SHMP resulted in blue-shifted spectra, indicating that the α-LA aggregated at pH 2.0. The details changes in wavelength maximum against every SHMP concentration were plotted in Table 1. The blue shift in wavelength maximum indicates that the Trp residues of α-LA moved into a more hydrophobic environment, which can be attributed to fluorophore internalization into the protein's hydrophobic core as a result of protein aggregate formation. In another study, it was found that the Trp residues internalized when concanavalin A formed aggregated after treatment with very low concentrations of cetyltrimethylammonium bromide (CTAB) at physiological pH[52].

To distinguish the nature of the aggregates formed in the presence of SHMP, specifically whether they adopt a fibrillar or amorphous structure, we employed two very important spectroscopic assays: ThT, CR dye binding, and far-UV CD. These assays are well known for probing the structural characteristics of protein aggregates in solution. ThT fluorescence is sensitive to the presence of β-sheet-rich fibrillar structures, making it an excellent indicator of amyloid formation[53]. Conversely, Congo Red dye binding relies on spectral shifts to detect the presence of ordered β-sheet structures, offering complementary insights into aggregate morphology[54]. Our results indicated that the aggregates formed in the presence of SHMP exhibited strong ThT binding, indicating the presence of β-sheet-rich fibrillar structures. Amyloid fibrillation was dependent on the SHMP concentration, as evidenced by the ThT signals, which increased proportionally to the SHMP concentration. Notably, the ThT signals reached saturation upon exposure to 1.0 mM SHMP, suggesting that a maximum level of fibrillation occurred at these concentrations. Additionally, we observed a notable spectral shift upon interaction with the CR dye, further suggesting the formation of ordered β-sheet structures within the aggregates. Another spectroscopic technique employed to characterize the nature of aggregates in solution was far-UV CD[55,56]. Typically, amyloid fibrils exhibit a characteristic of β-structure, which can be investigated through far-UV CD analysis. Our results indicated a profound alteration in the secondary structure of α-LA upon interaction with SHMP at acidic pH.

Under both acidic and physiological pH conditions, α-LA typically exhibits an alpha-helical secondary structure. However, in the presence of SHMP, the aggregated α-LA undergoes a structural transformation, converting its alpha-helical conformation into a β-structure. This structural transition was confirmed by observing a shift in the peak position of the far-far-UV CD spectra. Usually, α-LA exhibits two distinct peaks in far-UV CD spectra, with one peak observed at approximately 208 nm and the other at approximately 222 nm. However, upon interaction with SHMP, both of these characteristic peaks disappeared, while a new peak developed at 225 nm. This newly developed peak was indicative of a structural shift toward a β-structure conformation, distinguishing it from the original α-helical structure, and these peaks suggest that α-LA forms amyloid-like aggregates in the presence of SHMP. These types of far-UV CD spectral shifts were also recorded for other proteins in the presence of low concentrations of SDS detergents at low pH[57].

Conclusion

In summary, our study investigated the interaction mechanism between α-LA and SHMP at different pH levels. At acidic pH, α-LA forms amyloid-like aggregates in the presence of SHMP but remains soluble at physiological pH. The aggregation process is driven by both electrostatic and hydrophobic interactions, with the SHMP concentration playing a crucial role in determining the extent of aggregation. Our turbidity and kinetic data demonstrate the aggregation reaction is very rapid and reactions are concentration-dependent. The kinetic data suggest that once α-LA became aggregated in the presence of SHMP remained aggregated and turbidity as well as ThT fluorescence did not change for many days. Furthermore, changes in the intrinsic fluorescence spectra suggested structural alterations in α-LA upon interaction with SHMP, with Trp residues relocating to a more hydrophobic environment. Importantly, ThT, CR dye, and far-UV CD assays confirmed the presence of β-sheet-rich fibrillar structures in the aggregates, indicative of amyloid formation. These findings offer valuable insights into the potential impact of dietary phosphate additives on protein aggregation, underscoring the need for further research to elucidate their physiological implications and potential links to disease. Overall, our study enhances the understanding of the complex mechanisms underlying protein aggregation in food systems, contributing to broader discussions surrounding food safety and human health.

Data availability

All data generated or analyzed during this study are included in this published article.

Received: 23 May 2024; Accepted: 22 November 2024
Published online: 03 December 2024

References

1. Ritz, E., Hahn, K., Ketteler, M., Kuhlmann, M. K. & Mann, J. Phosphate additives in food—a health risk. *Dtsch. Arztebl Int.* **109**(4), 49–55 (2012).
2. Tian-Tian, Z., Xiao-Na, G. & Ke-Xue, Z. Effect of phosphate salts on the shelf-life and quality characteristics of semi-dried noodles. *Food Chem.* **384**, 132481 (2022).
3. Thayse, Y. H. et al. Effects of sodium hexametaphosphate and fluoride on the pH and inorganic components of Streptococcus mutans and Candida albicans biofilm after sucrose exposure. *Antibiotics (Basel)* **11**(8), 1044 (2022).
4. Thomas, E. R. et al. Hexametaphosphate as a potential therapy for the dissolution and prevention of kidney stones. *J. Mater. Chem. B* **8**(24), 5215–5224 (2020).
5. Robinson, T. E. et al. Local injection of a hexametaphosphate formulation reduces heterotopic ossification in vivo. *Mater. Today Bio.* **7**, 100059 (2020).
6. Weiner, M. L. et al. Toxicological review of inorganic phosphates. *Food Chem. Toxicol.* **39**, 759–786 (2001).
7. Cakar, M. et al. Findings of biopsyproven chronicity and end-stage renal failure associated with oral sodium phosphate solution. *Ren. Fail.* **34**, 499–501 (2012).
8. Maged, Y. et al. Re-evaluation of phosphoric acid–phosphates–di-, tri- and polyphosphates (E 338–341, E 343, E 450–452) as foodadditives and the safety of proposed extension of use. *EFSA J.* **17** (6), 5674 (2019).
9. Mehrdad, R., Soleiman, A., Fatemeh, A. & Rammile, E. On the heat stability of whey protein: Effect of sodium hexametaphosphate. *Int. J. Dairy. Technol.* **70**, 46–56 (2020).
10. Skelte, G. A. The effect of hexametaphosphate addition during milk powder manufacture on the properties of reconstituted skim milk. *Int. Dairy J.* **50**, 58–65 (2015).
11. Esther, K., Marcel, M., Thom, S., Toon, H. & Erik, V. L. Effect of calcium chelators on physical changes in casein micelles in concentrated micellar casein solutions. *Int. Dairy J.* **21**, 907–913 (2011).
12. Khurana, R. et al. A general model for amyloid fibril assembly based on morphological studies using atomic force microscopy. *Biophys. J.* **85**, 1135–1144 (2003).
13. Knowles, T. P. J., Vendruscolo, M. & Dobson, C. M. The amyloid state and its association with protein misfolding diseases. *Nat. Rev. Mol. Cell Biol.* **15**, 384–396 (2014).
14. Nelson, R. et al. Structure of the cross-β spine of amyloid-like fibrils. *Nature* **435**, 773–778 (2005).
15. Yong, Q. L. et al. Mechanisms of action of amyloid-beta and its precursor protein in neuronal cell death. *Metab. Brain Dis.* **35**, 11–30 (2020).
16. Andrea, A. et al. The infuence of cations on αlactalbumin amyloid aggregation. *J. Biol. Inorg. Chem.* **27**, 679–689 (2022).
17. Krissansen, G. W. Emerging health properties of whey proteins and their clinical implications. *J. Am. Coll. Nutr.* **26**, 713S–723S (2007).
18. Gang, W. et al. Self-assembling peptide and protein amyloids: from structure to tailored function in nanotechnology. *Chem. Soc. Rev.* **46**(15), 4661–4708 (2017).
19. Chiti, F. & Dobson, C. M. Protein misfolding, functional amyloid, and human disease. *Annu. Rev. Biochem.* **75**, 333–366 (2006).
20. Sania, B. et al. Trehalose restrains the fibril load towards α-lactalbumin aggregation and halts fibrillation in a concentration-dependent manner. *Biomolecules* **11**(3), 414 (2021).
21. Permyakov, E. A. & Berliner, L. J. α-lactalbumin: structure and function. *FEBS Lett.* **473**, 269–274 (2000).
22. Pellegrini, A. Antimicrobial peptides from food proteins. *Curr. Pharm. Des.* **9**, 1225–1238 (2003).
23. Nicoleta, S. et al. The novel therapeutic potential of bovine α-lactalbumin made lethal to tumour cells (BALMET) and oleic acid in oral squamous cell carcinoma (OSCC). *Eur. J. Cancer Prev.* **30**, 178–187 (2021).

24. Wijesinha-Bettoni, R., Dobson, C. M. & Redfield, C. Comparison of the denaturant-induced unfolding of the bovine and human α-lactalbumin molten globules. *J. Mol. Biol.* **312**, 261–273 (2001).
25. Rahamtullah, Rajesh, M. Nicking and fragmentation are responsible for α-lactalbumin amyloid fibril formation at acidic pH and elevated temperature. *Prot. Sci.* **30**, 1919–1934 (2021).
26. John, G., Sergei, E. P., Eugene, A. P., Vladimir, N. U. & Anthony, L. F. Conformational prerequisites for R-lactalbumin fibrillation. *Biochemistry* **41**, 12546–12551 (2002).
27. Bhanu, P. S., Ryan, J. M., Tilo, K., Cait, E. M. & Mathew, H. H. Lipid-induced polymorphic amyloid fibril formation by α-synuclein. *Protein Sci.* **32**(10), e4736 (2023).
28. Al-shabib, N. A. et al. Negatively charged food additive dye Allura Red rapidly induces SDS-soluble amyloid fibril in beta-lactoglobulin protein. *Int. J. Biol. Macromol.* **107**(Pt B), 1706–1716 (2018).
29. Kunihiro, K., Masamichi, I., Tatsuro, S., Yoshiki, H. & Shintaro, S. Kinetics of disulfide bond reduction in α-lactalbumin by dithiothreitol and molecular basis of superreactivity of the Cys6-Cys 120 disulfide bond. *Biochemistry* **29**, 8240–8249 (1990).
30. Javed, M. K. et al. Protonation favors aggregation of lysozyme with SDS. *Soft Matter* **10**, 2591 (2014).
31. Ahmad, E., Rahman, S. K., Khan, J. M., Varshney, A. & Khan, R. H. Phytolaccaamericana lectin (Pa-2; pokeweed mitogen): an intrinsically unordered protein and its conversion in to partial order at low pH. *Biosci. Rep.* **30**, 125–134 (2010).
32. Nasser, A. A. et al. Molecular insight into binding behavior of polyphenol (rutin) with beta lactoglobulin: Spectroscopic, molecular docking and MD simulation studies. *J. Mol. Liq.* **269**, 511–520 (2018).
33. Marcus, D. H. et al. Avogadro: an advanced semantic chemical editor, visualization, and analysis platform. *J. Cheminform.* **4**, 17 (2012).
34. O'Boyle, N. M. et al. Open Babel: an open chemical toolbox. *J. Cheminform.* **3**, 33 (2011).
35. AlAjmi, M. F., Rehman, M. T., Hussain, A. & Rather, G. M. Pharmacoinformatics approach for the identification of Polo-like kinase-1 inhibitors from natural sources as anti-cancer agents. *Int. J. Biol. Macromol.* **116**, 173–181 (2018).
36. Rehman, M. T., Shamsi, H. & Khan, A. U. Insight into the binding mechanism of imipenem to human serum albumin by spectroscopic and computational approaches. *Mol. Pharm.* **11**(6), 1785–1797 (2014).
37. Rehman, M. T., Ahmed, S. & Khan, A. U. Interaction of meropenem with 'N' and 'B' isoforms of human serum albumin: a spectroscopic and molecular docking study. *J. Biomol. Struct. Dyn.* **34**(9), 1849–1864 (2016).
38. Nasser, A. A. et al. Molecular interactions of food additive dye quinoline yellow (qy) with alpha-lactalbumin: Spectroscopic and computational studies. *J. Mol. Liq.* **311**, 113215 (2020).
39. Yamazaki, M., Ikeda, K., Kameda, T., Nakao, H. & Nakano, M. Kinetic mechanism of amyloid-β-(16–22) peptide fibrillation. *J. Phys. Chem. Lett.* **13**, 6031–6036 (2022).
40. Ghahghaei, A., Divsalar, A. & Faridi, N. The effects of molecular crowding on the amyloid fibril formation of a-lactalbumin and the chaperone action of a-casein. *Protein J.* **29**, 257–264 (2010).
41. Dobenecker, B., Reese, S. & Herbst, S. Effects of dietary phosphates from organic and inorganic sources on parameters of phosphorus homeostasis in healthy adult dogs. *PLoS One* **16**(2), e0246950 (2021).
42. Barcenilla, C., Alvarez-Ordonez, A., Lopez, M., Alvseike, O. & Prieto, M. Microbiological safety and shelf-life of low-salt meat products—a review. *Foods* **11**(15), 2331 (2022).
43. Khan, J. M., Malik, A., Ahmed, A., Alghamdi, O. H. A. & Ahmed, M. SDS induces cross beta-sheet amyloid as well as alpha-helical structure in conconavalin A. *J. Mol. Liq.* **319**, 114154 (2020).
44. Olofsson, A., Borowik, T., Gröbner, G. & Sauer-Eriksson, A. E. Negatively charged phospholipid membranes induce amyloid formation of Medin via an α-Helical Intermediate. *J. Mol. Biol.* **374**, 186–194 (2007).
45. Yamaguchi, K., Nakajima, K. & Goto, Y. Mechanisms of polyphosphate-induced amyloid fibril formation triggered by breakdown of supersaturation. *Biophys. Physicobiol* **20**(1), e200013 (2023).
46. Marshall, K. E. et al. Hydrophobic, aromatic, and electrostatic interactions play a central role in amyloid fibril formation and stability. *Biochemistry* **12**, 2061–2071 (2011).
47. Malik, A., Khan, J. M., Alhomida, A. S. & Ola, M. S. Perturbation of surfactant-induced amyloids by abolishing electrostatic interactions. *J. Mol. Liq.* **385**, 122440 (2023).
48. Malik, A. et al. Hexametaphosphate, a common food additive, aggregated the hen egg white lysozyme. *ACS Omega* **8**, 44086–44092 (2023).
49. Malik, A. et al. A common food additive (E452), hexametaphosphate, denatures the digestive enzyme trypsin. *J. King Saud Univ. Sci.* **35**, 102968 (2023).
50. Morris, A. M. & Watzky, M. A. Protein aggregation kinetics, mechanism, and curve-fitting: a review of the literature. *Biochim. Biophys. Acta Proteins Proteom.* **1794**, 375–397 (2009).
51. Khan, J. M., Malik, A. & AlAmri, A. M. Gel tracking dye bromophenol blue promote amorphous aggregation in insulin. *J. Mol. Liq.* **385**, 122417 (2023).
52. Khan, J. M., Khan, M. S., Ali, M. S., Al Shabib, N. A. & Khan, R. H. Cetyltrimethylammonium bromide (CTAB) promote amyloid fibril formation in carbohydrate binding protein (concanavalin A) at physiological pH. *RSC Adv.* **6**, 38100 (2016).
53. Biancalana, M. & Koide, S. Molecular mechanism of Thioflavin-T binding to amyloid fibrils. *Biochim. Biophys. Acta.* **1804**(7), 1405–1412 (2010).
54. Espargaro, A. et al. On the binding of Congo Red to amyloid fibrils. *Angew Chem. Int. Ed.* **59**, 1–5 (2020).
55. Skamris, T., Marasini, C., Madsen, K. L., Fodera, V. & Vestergaard, B. Early stage alpha-synuclein amyloid fibrils are reservoirs of membrane-binding species. *Sci. Rep.* **9**, 1733 (2019).
56. Clara, I. et al. Vanillin affects amyloid aggregation and non-enzymatic glycation in human insulin. *Sci. Rep.* **7**, 15086 (2017).
57. Khan, J. M. et al. The Achilles' heel of ultrastable hyperthermophile proteins: submillimolar concentrations of SDS stimulate rapid conformational change, aggregation, and amyloid formation in proteins carrying overall positive charge. *Biochemistry* **55**, 3920–3936 (2016).

Acknowledgements

The authors are grateful to the Researchers Supporting Project Number RSPD2024R923, King Saud University, Riyadh, Saudi Arabia.The authors are thankful to university of Helsinki for open access support.

Author contributions

Nasser Abdulatif Al-Shabib: Conceptualization; data curation; formal analysis; funding acquisition; investigation; methodology; supervision; roles/writing—original draft; writing—review and editing. Javed Masood Khan: Conceptualization; data curation; formal analysis; funding acquisition; investigation; methodology; project administration; Resources; software; supervision; validation; roles/writing—original draft; writing—review and editing. Ajamaluddin Malik: Investigation; methodology; resources; software; validation; roles/writing—original draft; writing—review and editing. Md Tabish Rehman: Investigation; methodology; resources; software; validation; writing—review and editing. Abdulaziz Alamri: Investigation; methodology; resources; software; validation. Vijay Kumar: Validation; writing—review and editing. Per Erik Joakim Saris: Validation; writing—

review and editing. Fohad Mabood Husain: Investigation; methodology. Mohamed F. AlAjmi: Investigation; methodology; resources; software; validation.

Declarations

Competing interests
The authors declare no competing interests.

Additional information
Correspondence and requests for materials should be addressed to N.A.A.-S., J.M.K. or P.E.J.S.

Reprints and permissions information is available at www.nature.com/reprints.

Publisher's note Springer Nature remains neutral with regard to jurisdictional claims in published maps and institutional affiliations.